DESIGN OF 4D LANDING APPROACH TRAJECTORIES FOR A QUIET STOL AIRPLANE

O. Macke and R. Koenig
DLR – German Aerospace Center, Institute of Flight Systems
Lilienthalplatz 7, 38108 Braunschweig, Germany

Keywords: *aircraft noise, approach procedure, trajectory design, STOL, powered lift*

Abstract

The advent of new, satellite-based navigation technologies enables the use of 4D trajectories, including precise altitudes and times at all waypoints ahead to touchdown. A better management of arrival times of aircraft at airports will enable the use of shorter, cleaner and quieter trajectories. To affect arrival times without lengthening the ground track, varying glideslope angles can be used. For aircraft equipped with powered lift, the glideslope angle has an impact on achievable landing speeds. Landing approach performance parameters such as possible flight path angles or minimum airspeeds are calculated for an aircraft with upper surface blowing. These are used to simulate landing approaches using different glideslope angles. Flight durations and noise level contour areas are compared for different glideslope angles. Increasing glideslope angles results in significant reductions of both.

List of Symbols, Abbreviations and Acronyms

C	Coefficient
$CONF$	Configuration setting
D	Drag
L	Lift
L_{Amax}	Maximum A-weighted sound pressure level
M	Mach number
PL	normalized power lever angle
T	Thrust
V	Airspeed
W	Weight
X	Distance to touchdown
Y	Lateral distance to flight track
g	Acceleration due to gravity
m	Mass
Δ	Difference
Θ	Pitch angle
α	Angle of attack
γ	Flight path angle

CAS	Calibrated airspeed
Cmd	Command
DLR	German Aerospace Center
GLS	GNSS landing system
GNSS	Global navigation satellite system
ICAO	International Civil Aviation Organization
ILS	Instrument landing system
LDLP	Low drag low power approach
max	Maximum
min	Minimum
RNAV	Area navigation
Sim	Simulation
STOL	Short takeoff and landing
USB	Upper surface blowing

1 Introduction

For short trips via aircraft, large parts of the travel time are made up of the travels to and from large airports. These travel times could be reduced by using smaller community airports that are close to large and medium-sized cities. But small airports can not be used by modern, high performance aircraft due to their need for relatively long runways. Aircraft newly designed to use these airports would have to operate very quietly to become accepted by the residents living near the airports.

The German Aerospace Center (DLR) is performing studies for a quiet, 150 passenger

aircraft capable of short take-off and landing (STOL). It is planned to achieve the capability to use runways not longer than 900 m by the use of upper surface blowing (USB). This is a form of powered-lift in which the jet of engines mounted on top of the wings increases lift [1], which in turn reduces minimum flight speeds depending on thrust. This leads to a reduction of necessary runway lengths. Fig. 1 shows an Antonow An-72 as an example of a USB aircraft.

Fig. 1. Antonow An-72 as an example USB aircraft. Copyright Sergey Chernyshov, used with permission

The studies include the analysis of aircraft noise radiation in the preliminary design stage [2]. But in order to design an exceptionally quiet aircraft, the optimization of trajectories is as important as minimizing noise sources on the aircraft itself. Successful designs of noise abatement procedures have been shown e.g. in references [3] - [6].

To reduce noise impact on the ground, steep approaches are analyzed in this paper, as these show high potential in reducing aircraft noise [7]. Approaches with different glideslope angles are compared regarding noise contour areas and flight times. A use of different approach procedures with varying glideslope angles and accurate knowledge of the flight times associated with each procedure (4D trajectories, the four dimensions being the three-dimensional position in space plus time) will enable air traffic controllers to delay single aircraft by assigning them approach procedures with longer flight times. This way, noisy holding patterns may be avoided. Individual aircraft would in fact use suboptimal glideslope angles regarding the noise of a single approach, but for a multiple-aircraft scenario, these approaches would be quieter than holding patterns. An implementation of different, ILS-independent glideslopes is made possible using navigation by global navigation satellite systems such as RNAV and GLS [8].

For noise level calculation/simulation, the SIMUL software [9] of the German Aerospace Center was used, which was introduced in 1988. This software has been enhanced continuously. SIMUL is based on a separate modeling of engine and airframe noise sources and accounts for directional characteristics as well as for spectral information. This spectral information is used for calculating the A-weighted maximum sound pressure level L_{Amax} along simulated flight paths. This level is used in accordance with Federal Aviation Agency policy to use it “as the single event maximum sound level metric” [10]. Having calculated the sound pressure levels along the simulated flight paths, contours of equal L_{Amax} are drawn and their area calculated.

In the current version of SIMUL only noise emission calculations for the Airbus A320 aircraft can be performed. While the use of this software will lead to errors in absolute sound pressure level for the STOL aircraft, a comparison of the noise level contour areas of different approach procedures is likely to produce fairly good results. The interaction of the exhaust jet with the flap trailing edge will lead to higher noise than calculated, underestimating the influence of thrust on noise. This will be partially compensated by the shielding of the jets by the wing.

2 Aerodynamics and Engine

2.1 Aerodynamics

Preliminary design methods were used to calculate the aerodynamics of an aircraft similar to the Boeing YC-14 experimental aircraft [11]. This technology demonstrator was equipped with two engines delivering USB to inboard double-slotted trailing-edge flaps. The outboard flaps were also double-slotted, and the aircraft had full-span leading-edge Krueger flaps with boundary layer control (blowing of engine bleed air, also called internally blown

flaps). The different flap settings used in this study (clean, landing approach, and landing) are numbered from 0 to 2 and are broken down in Table 1. Wing and tail geometry is shown in Table 2.

Table 1. Flap angles for the configuration settings

CONF No.	descrip-tion	USB flap deflection	outboard flap deflection	Krueger flaps
0	clean	0°	0°	retracted
1	landing approach	30°	30°	extended
2	landing	50°	60°	extended

With these measures, very high angles of attack and very high lift coefficients were reached in flight tests [12]. However, high angles of attack caused high rates of descent due to the associated high drag. Because of that, a stick shaker warned the pilots against unsafe flight conditions when reaching α = 32° or $\dot{H}$ = -12.7 m/s (-2500 ft/min) [13]. The lowest airspeed reached in flight was V = 30 m/s [12].

Table 2. Wing and tail geometry [11]

	wing	**horizontal tail**	**vertical tail**
area	163.7 m²	56.0 m²	48.1 m²
span	39.3 m	16.7 m	7.0 m
aspect ratio	9.44	5.00	1.03
taper ratio	0.35	0.50	1.00
sweep	4.87°	3.51°	25.00°
rel. airfoil thickness	0.16 to 0.12	0.12	0.13
dihedral	0°	-4°	-

The preliminary design methods account for the aerodynamics of the basic wing using lifting line methods [14], and for the high-lift devices using handbook methods [15]. The additional pressure on the profile upper surface due to the deflection of the engine jet is calculated using the circular streamline theory [16], and the jet-flap effect using Ref. [17]. The jet-flap effect describes the tendency of the jet to act as an extension of the existing flap, thus increasing its efficiency.

The resulting aerodynamic model describes the coefficients of lift (C_L), drag (C_D) and thrust (C_T) as a function of normalized power lever angle (*PL*), angle of attack (α), Mach number (*M*) and configuration setting (*CONF*). Fig. 2 shows the lift coefficient vs. power lever and angle of attack for the landing configuration at *M* = 0.2. Lift coefficients of up to 6.0 can be reached at full thrust (PL = 1) and maximum angle of attack (α_{max} = 32°).

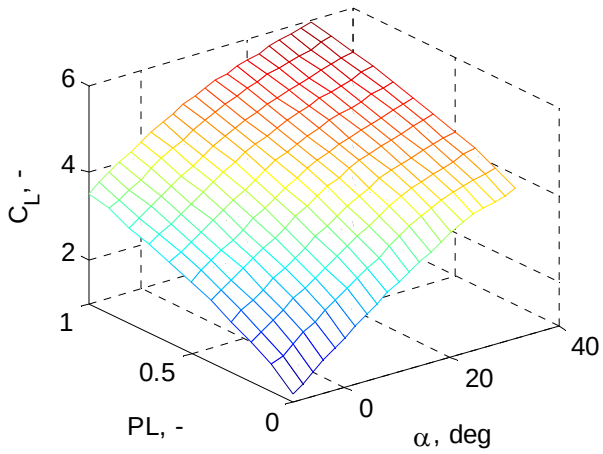

Fig. 2. Lift coefficient vs. power lever angle and angle of attack for landing configuration at *M* = 0.2

The lift vs. drag curves for different configurations with idle engines can be seen in Fig. 3. The figure shows the characteristic quadratic drag polar for each configuration. Higher configuration settings lead to higher parasitic drag and higher maximum lift coefficients. The high maximum lift coefficients at all configurations result from the internally blown Krueger flaps. The gear increases drag.

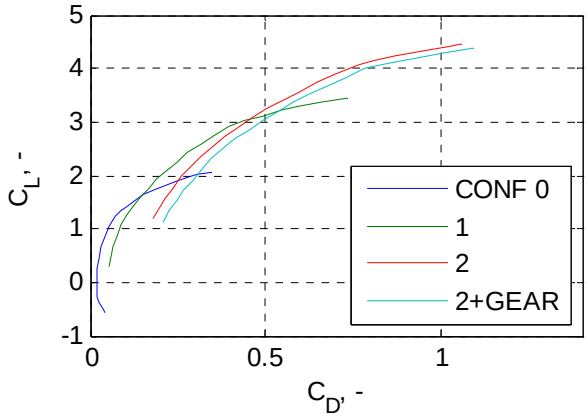

Fig. 3 Lift vs. drag curves for different configurations with idle engines at *M* = 0.2

2.2 Engine

The engines used for the YC-14 were two General Electric CF6-50D. Data for this engine can be found in Table 3. Necessary data to calculate the upper surface blowing aerodynamics, such as jet velocity behind the engine, were calculated using Ref. [19]. In the performed simulations, engine dynamics were approximated by a first-order time-delay with a time constant of three seconds.

Table 3. Engine data [11], [18]

engine type	General Electric CF6-50D
static thrust	217 kN
air mass flow	670 kg/s
bypass ratio	4.3
fan pressure ratio	1.71
compressor pressure ratio	30.4
turbine entry temperature	1565 K

3 Performance

The fundamental equation for landing approach performance is (1). With this equation, maximum and minimum flight path angles (γ_{max} and γ_{min}) for non-accelerated flight ($\dot{V} = 0$), maximum and minimum accelerations ($\dot{V}_{max}$ and $\dot{V}_{min}$) for level flight ($\gamma = 0$) or a combination of both can be calculated as a function of thrust to weight (T / W) and drag to lift ratios (C_D / C_L).

$$\sin\gamma + \frac{\dot{V}}{g} = \frac{T}{W} - \frac{C_D}{C_L} \qquad (1)$$

For the performance studies in this paper, only minimum flight path angles for non-accelerated flight are shown at different speeds and different weights.

The knowledge of minimum speeds V_{min} for each configuration setting is also important for the design of landing approach trajectories. Minimum speeds are defined in FAR Part 25 as multiples of the reference stall speed V_{SR}. The reference stall speed is the speed at maximum lift coefficient and is thus dependent on aircraft weight. While takeoff must be performed at least at $1.13 \cdot V_{SR}$, $1.23 \cdot V_{SR}$ is the minimum speed for landing. For safety reasons, this factor is increased to 1.3 for clean and landing approach configurations in this study. The minimum speeds influence the flap scheduling and the landing speeds. Landing speeds in turn influence the required runway distances, which are inherently important for STOL aircraft.

3.1 Minimum Flight Path Angles

To design steep approaches, knowledge of the steepest flight path angle achievable with idle engines and without accelerating is necessary. It depends on the thrust of idle engines, the aircraft weight, and the ratio of drag to lift (equation 1). Drag and lift in turn depend on airspeed, angle of attack and position of flaps, slats and gear, i.e. the configuration setting.

Minimum flight path angles for different weights are shown in Fig. 4. The airspeed is set to 5 m/s above the minimum speed to assume a typical flight speed. As can be seen the angles are steeper for higher configuration settings, resulting from a larger drag to lift ratio (cf. Fig. 3).

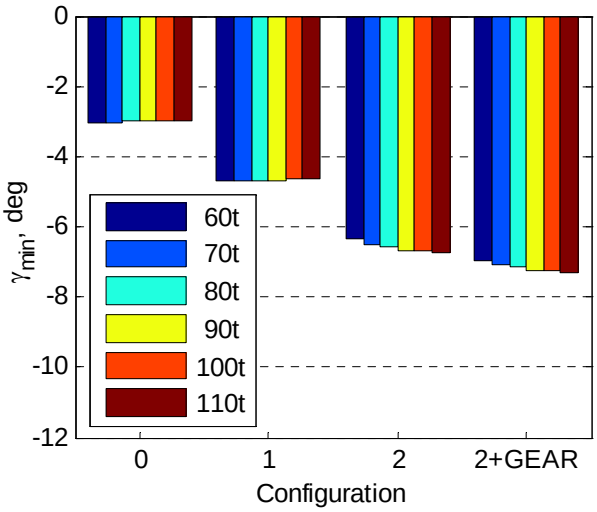

Fig. 4. Minimum flight path angle with idle engines for different weights at V_{min} + 5 m/s

Remarkably, the flight path angles are nearly constant with varying weight. This can be explained with the help of equation (1): Minimum flight path angles are dependent on thrust to weight and drag to lift ratios. On the one hand, weight-dependent minimum speeds are characterized by nearly constant lift coefficients and thus nearly constant drag coefficients for a given configuration; i.e. the ratio of drag to lift stays constant. On the other

hand, the influence of changing weight is almost negligible, as the ratio of thrust to weight is almost zero with idle engines.

If the airspeed is not changed with weight as would be the case e.g. for a 250 kt descent, minimum flight path angles do change with weight, a larger weight leading to a steeper angle (not shown).

The influence of airspeed on minimum flight path angles with idle engines can be seen in Fig. 5. A mass of 70 metric tons was selected as a typical landing weight, compared to the maximum take-off weight of 110 metric tons of the analyzed aircraft. The curve for each configuration ranges from minimum speed to maximum allowable speed. The speed for clean configuration is limited by the maximum allowed airspeed of 129 m/s (250 kt) below an altitude of 3048 m (10 000 ft) due to ICAO recommendations. For higher configuration settings, the maximum speeds are limited by allowable flap loads.

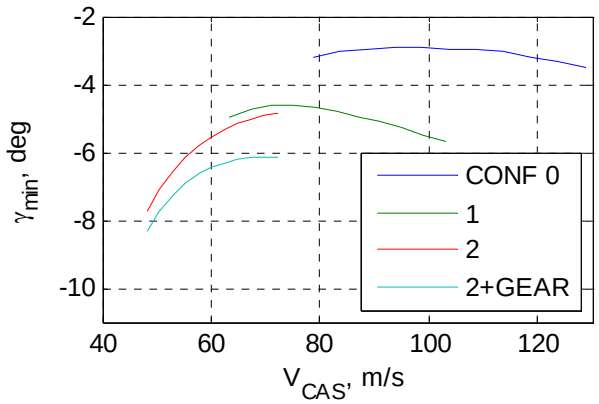

Fig. 5. Minimum flight path angle with idle engines for different airspeeds at m = 70 t

For the configuration settings 0 and 1, the minimum flight path angles change only slightly with airspeed. For configuration 2 however, the angle decreases significantly with decreasing airspeed. The reasons for this behavior are the increasing ratios of C_D / C_L for increasing configuration settings and for increasing lift coefficient. The required lift coefficient is inversely proportional to the square of airspeed (i.e. $C_L \propto 1/V^2$) and the drag coefficient rises approximately quadratically with the lift coefficient, so C_D is a function of $1/V^4$. The differences in C_L versus C_D between configuration settings 1 and 2 are increased by the fact that the minimum speeds are calculated with different stall speed margins. While the minimum speed for configuration 1 is calculated as $1.3 \cdot V_{SR}$, the minimum speed for configuration 2 is the target speed for landing and is calculated as $1.23 \cdot V_{SR}$ (see above).

3.2 Minimum Airspeeds

To design an approach procedure, the minimum flight speeds for each configuration must be known. For a conventional aircraft, the minimum speeds are only a function of weight, while for an aircraft with powered-lift, the maximum lift coefficients and therefore the minimum speeds are dependent on thrust setting. But the thrust can not be set independently from flight path angle and acceleration / deceleration (equation 1). To obtain the minimum airspeeds versus flight path angle for a non-accelerated climb or descent at minimum speed, trimming calculations were performed. Setting different thrust and appropriate minimum speeds resulted in corresponding flight path angles (Fig. 6).

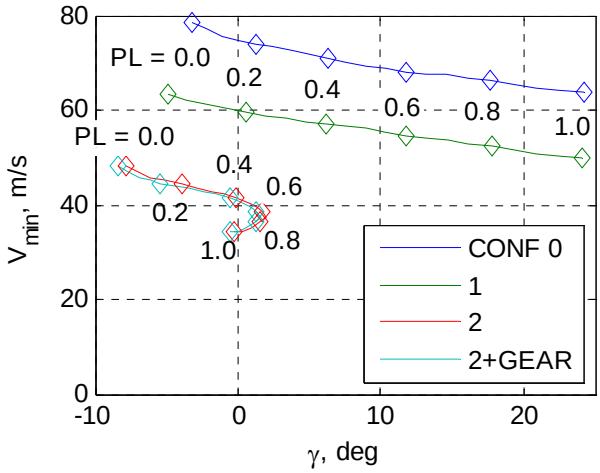

Fig. 6. Minimum airspeeds for different flight path angles at m = 70 t

As could already be seen in Fig. 5, lower airspeeds are possible with higher configuration settings. With the mass of 70 metric tons, very high flight path angles of 24 degrees are possible at full thrust for configurations 0 and 1. For configuration 2, with and without gear, the angles are considerably lower because of

the high drag of this configuration. The minimum achievable flight path angles are obtained with idle engines and could also already be observed in Fig. 5.

The minimum airspeeds decrease for higher flight path angles and thus higher thrust settings, as was expected. These varying minimum speeds must be considered for steep approaches. In clean configuration, minimum speed decreases from 79 m/s for idle thrust to 64 m/s for full thrust, a reduction by 19 %. The decrease for approach configuration is from 63 to 50 m/s, or by 20 %, and for landing configuration from 48 to 34 m/s, or by 29 %.

For CONF 2 and for power lever angles larger than 0.7, the possible flight path angle at minimum airspeed begins to decrease. This is because the ratio of drag to lift increases more than the ratio of thrust to weight at the minimum airspeed associated with the power lever setting (equation 1). This has also been observed previously for other powered-lift configurations [20], [21]. Because it would be impossible to reach the minimum speed for these power lever settings without performing complicated maneuvers, the minimum airspeed for power lever settings larger than 0.7 is set to 38 m/s. This airspeed results in flight path angles of 2.3° and 3.8° for power lever settings of 0.8 and 1.0, respectively, for configuration 2, and 2.1° and 4.4° for configuration 2 with gear.

4 Procedures

Simulations of the approaches were carried out with no wind and on straight tracks to obtain generic, airport-independent approaches. These simulations can be conducted for airport-specific, curved approach trajectories to provide similar results. In order to carry out the simulations, controllers were designed to replicate the functions of modern flight management systems and autopilots.

4.1 Standard Procedure

The established standard procedure for landing approaches is the low drag low power (LDLP) approach. As an example of an LDLP approach, Lufthansa's "noise abatement ILS approach" has completely replaced the old "ILS approach" in the operations manuals of the German airline between 1998 and 2001. The name comes from a late extension of the landing gear and of the flaps to landing configuration, resulting in low drag. Because of the low drag, the aircraft can be flown longer with idle engines (low power) while decelerating on the glideslope, reducing noise. The standard glideslope angle for ILS approaches is 3°.

The LDLP procedure will be described subsequently for the STOL aircraft (Fig. 7). The figure shows simulated and commanded values for height, flight path angle and calibrated airspeed, as well as maximum and minimum allowed airspeeds dependent on configuration setting. Also shown are angle of attack, pitch angle, configuration and gear setting, thrust and normalized power lever angle.

The procedure begins with a level flight at an altitude assigned by air traffic control, and at a maximum calibrated airspeed of 129 m/s (250 kt), which is the maximum allowed by ICAO recommendations below an altitude of 3048 m (10 000 ft). In this study, an altitude of 2133 m (7000 ft) and a calibrated airspeed of 129 m/s are chosen as typical values. Starting at these values, the aircraft performs an "open descent", which is characterized by idle thrust setting and constant speed. This results in a certain (open) flight path angle, which is dependent on the aircraft weight, idle thrust, aerodynamics and wind. Because a flight path angle is not explicitly required, no commanded values for the flight path angle and the height are plotted for the open descent segment.

Arriving at the intermediate approach altitude, typically 914 m (3000 ft), a change to level flight takes place. To reduce speed for landing, a deceleration is necessary, and lower speeds require the extension of flaps and slats to maintain lift. Therefore, the first configuration setting has to be engaged when reaching the minimum speed for clean configuration. A three degrees glideslope will be intercepted from below at about 17 km distance from touchdown. On glide path, the aircraft decelerates further until the minimum

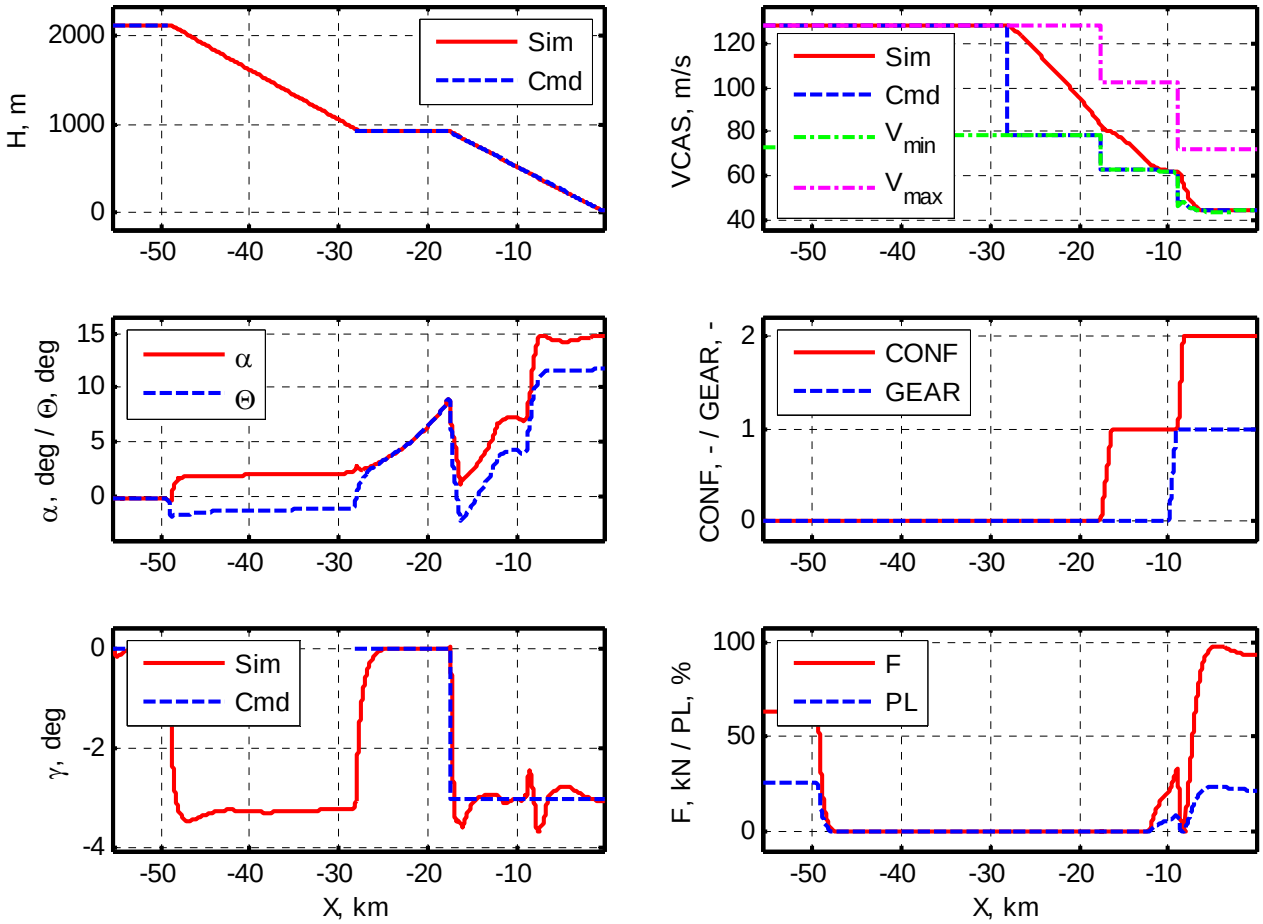

Fig. 7. Simulated LDLP approach with a glideslope angle of 3°

speed for configuration 1 is reached. At this point, thrust is adapted to maintain airspeed. At about 488 m (1600 ft) above ground, the landing gear will be extended, directly followed by a configuration change to setting 2. The aircraft decelerates to landing speed, again adapting thrust. The aircraft has reached landing speed at about 335 m (1100 ft) height above ground.

Fig. 8 shows an enlarged view of airspeed vs. distance. The change of minimum airspeed with thrust setting can be identified. The landing speed is reduced from 48 to 44 m/s by the thrust increase. This is a reduction of the kinetic energy by 16 %, which will reduce the landing distance.

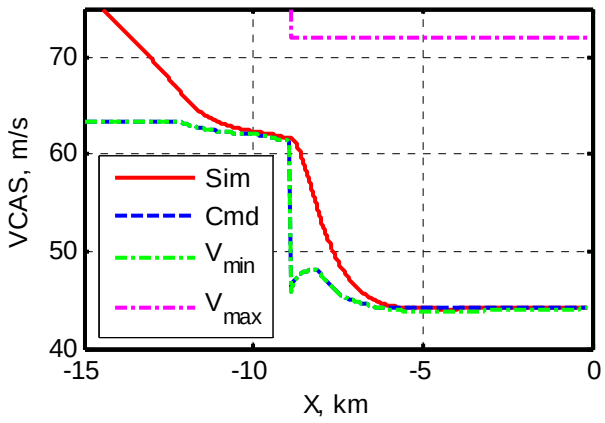

Fig. 8: Larger view of airspeed vs. distance; influence of thrust on minimum speed and reduction of landing speed

Shown in Fig. 9 are the contours of maximum A-weighted sound pressure level L_{Amax}. The outermost contour is the 55 dB-contour, the next 60 dB, etc., each color step representing a change of 5 dB. The 65 dB-island at 30 km before touchdown results from the descent to the intermediate approach

altitude (less altitude meaning more noise), followed by a decrease of airspeed (less airspeed meaning less noise). The second rise above 65 dB originates from the extension of slats and flaps to configuration setting 1, the slats being one of the largest noise sources on an aircraft apart from the engines.

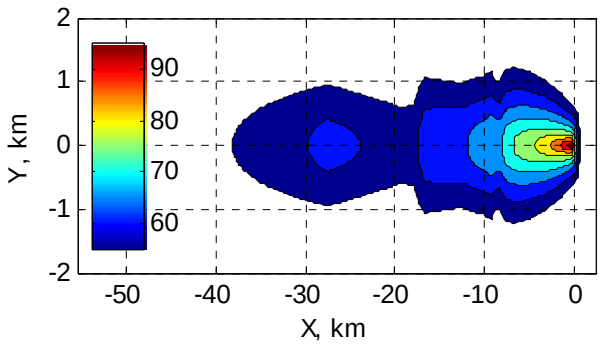

Fig. 9. Contours of A-weighted sound pressure level

4.2 Steep Approaches

Glideslope angles of up to 5° are possible with the studied aircraft for an optimized approach with late stabilization, at which point a rate of descent of 4.1 m/s (800 ft/min) is reached. Higher glideslope angles would be possible at the maximum allowed rate of descent of 5.1 m/s (1000 ft/min) and a landing speed of 48 m/s (up to 6°), but only with operational constraints such as extending gear and setting configuration 2 already on the intermediate approach altitude. The resulting high drag and thus high deceleration would require thrust setting on the intermediate approach altitude and early on the glideslope to ensure minimum speeds not being undershot, hence actually increasing noise on the ground in these areas compared to approaches with a smaller glideslope angle.

Approaches with glideslope angles of 3° to 5° with steps of 0.5° are shown in Fig. 10.

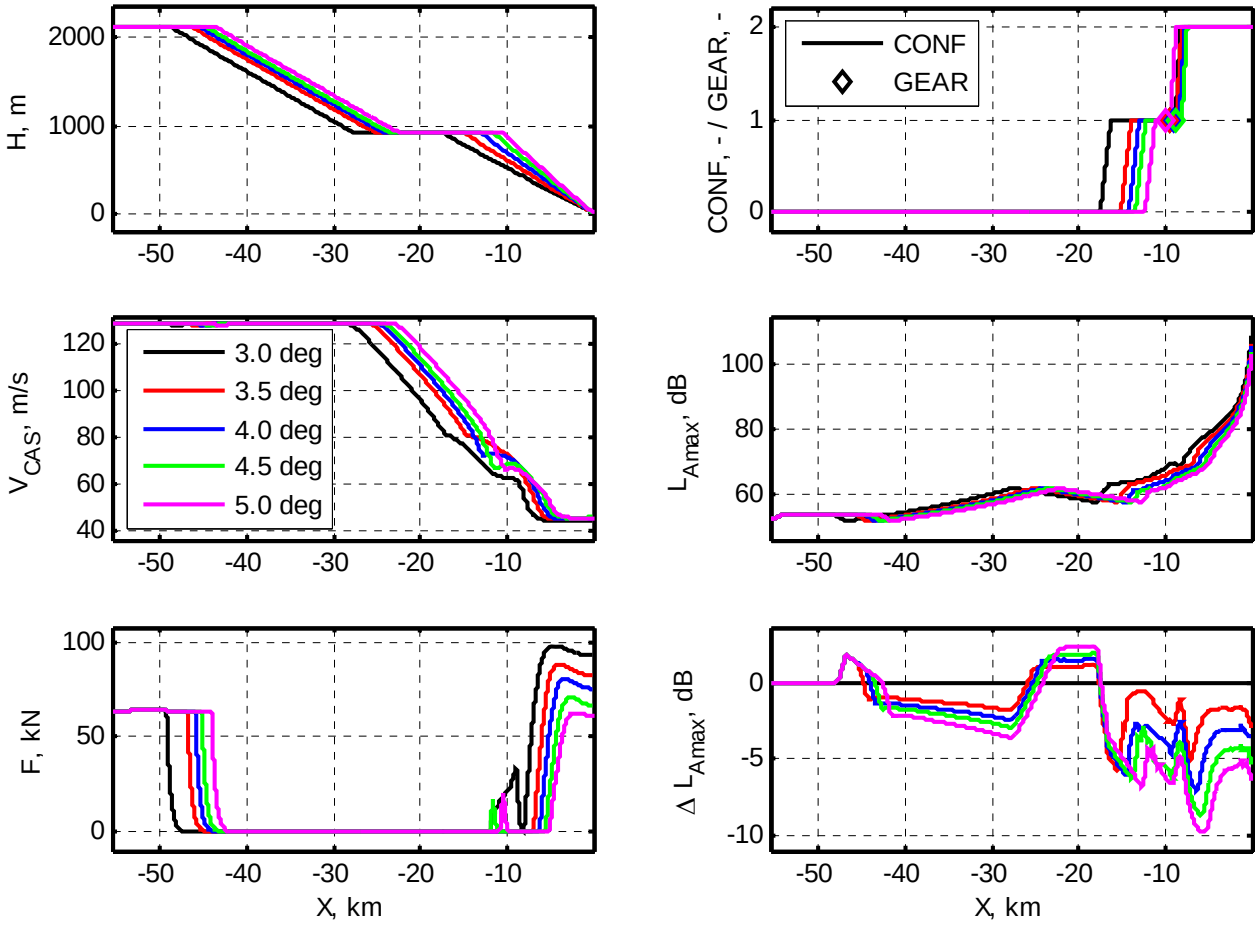

Fig. 10. Simulated LDLP approaches with different glideslope angles

The approach with 3° was already described above. For higher angles, the point of descent is moved closer to the airport, because the glideslope capture takes place closer to the airport. All approaches reach landing speed at the same height, approximately 335 m (1100 ft) above ground. Because the deceleration decreases for higher glideslope angles and constant configuration settings (equation 1), the constant stabilization height is achieved by extending the gear and changing to configuration 2 at increasing altitudes. But in combination with the rising glideslope angle, this leads to an extension at approximately the same distance from the touchdown point. The exception is the approach with 5°, where the gear is already extended on glideslope capture to prevent a speed increase.

Due to the lower flight path angles at higher glideslope angles, the thrust necessary for maintaining landing speed is reduced. The combination of greater height, lower thrust and later change to configuration 1 leads to a decrease of L_{Amax} under the flight path, as can also be seen in Fig. 10. The approach with 5° leads to a difference in sound pressure level (ΔL_{Amax}) under the glide path of 5 to 10 dB compared to the 3°-approach.

The landing speed rises from 44 m/s at 3° to 45 m/s at 5°. This is a 5 % increase in kinetic energy (affecting needed runway length), but still a 12 % decrease compared to the minimum speed with idle engines, 48 m/s.

4.2.1 Aircraft Noise Evaluation

Fig. 11 shows a comparison of the contours of different maximum A-weighted sound pressure levels for the different glide path angles. As can be seen, the contour areas of all noise levels are reduced in size for growing glideslope angles. Even the early extension of the gear for the 5°-approach has no noticeable negative effect on noise reduction.

The changes of the contour areas are made evident in Fig. 12. Especially the contour areas of higher sound pressure levels are influenced by changes of the glideslope angle. For a 5°-approach, a reduction by 42 % is possible for the contour areas of sound pressure levels greater than 65 dB. For a 4°-approach, a reduction of more than 26 % is possible.

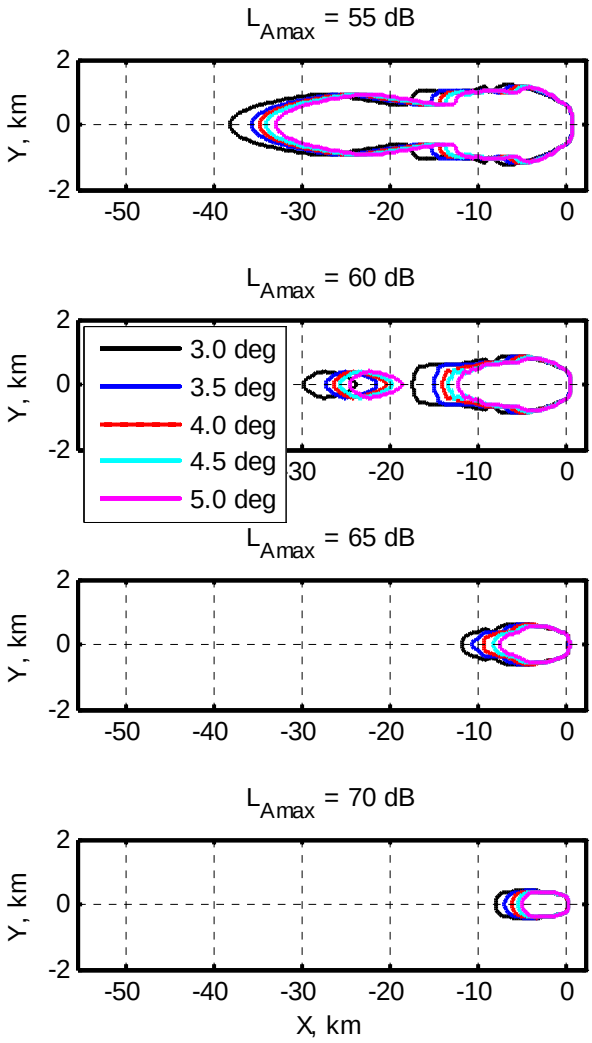

Fig. 11 Comparison of the contours of maximum A-weighted sound pressure level for steep approaches

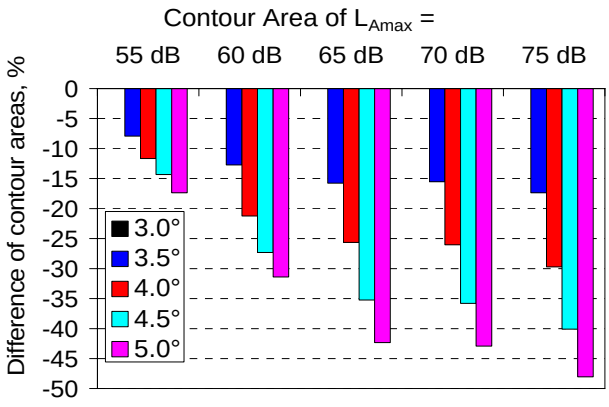

Fig. 12. Comparison of the contour areas for different glideslope angles

4.2.2 Evaluation of flight time

Important for planning approaches are the flight times of the different procedures from a certain point until touchdown. The total flight time for the simulated distance of 55 km to touchdown and the flight time for final approach (the time spent on the glideslope) are shown in Fig. 13. Total flight time can be reduced from 599 seconds to 544 seconds, i.e. by 55 seconds or 9 %. This is almost half the time of a standard 2-minute-turn and should provide sufficient time for controllers to avoid holding patterns at little frequented community airports. As stated above, the glideslope angle can not be used to reduce the noise of a single approach if it is used to control flight time. Instead, the total noise of the scenario is reduced by eliminating holding patterns.

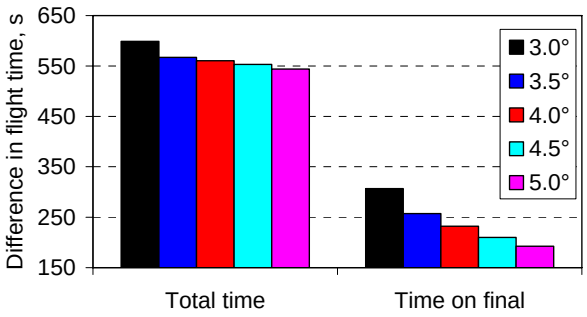

Fig. 13. Comparison of the total flight time and the flight time on final approach for different glideslope angles

For the merging of aircraft traffic from different directions to create correct spacing between them, the time spent on final approach is important. As the merging has to be complete before the aircraft reach the glideslope, a short time spent on final approach has a positive effect on planning freedom. This time can be shortened from 307 seconds to 193 seconds, a reduction by 114 seconds or 37 %.

5 Conclusions and Outlook

Low drag low power approach procedures with different glideslope angles were simulated for an upper surface blowing aircraft. Large reductions of the noise level contour areas calculated using maximum A-weighted sound pressure level can be achieved with higher glideslope angles.

More freedom for approach planning is possible through shorter final approaches by creating 4D landing approach trajectories with higher glideslope angles. Holding patterns can be avoided by lengthening flight time using approaches with a smaller glideslope angle. To achieve this, approach procedures with different glideslopes will have to be implemented in the flight management systems of aircraft. These ILS-independent glideslopes are made possible using navigation by global navigation satellite systems such as RNAV and GLS.

More research will be conducted on this subject. In particular, new noise prediction models for upper surface blowing are being developed from acoustic wind tunnel testing. Furthermore, an aircraft model better suited for 150 passengers than the Boeing YC-14 is designed.

Acknowledgements

The authors would like to thank Lothar Bertsch and Thomas Kehse of the DLR Institute of Aerodynamics and Flow Technology for providing the aerodynamics of the studied aircraft.

References

[1] Lan C E and Campbell J F. *Theoretical aerodynamics of upper-surface-blowing jet-wing interaction.* NASA-TN-D-7936, 1975.

[2] Bertsch L, Dobrzynski W and Guérin S. Tool Development for Low-Noise Aircraft Design, *Proc. 14th AIAA/CEAS Aeroacoustics Conference*, paper no. AIAA-2008-2995, Vancouver, British Columbia, Canada, 2008

[3] Clarke J P B. Systems Analysis of Noise Abatement Procedures Enabled by Advanced Flight Guidance Technology. *Journal of Aircraft*, Vol. 37, No. 2, pp 266-273, 2000

[4] Clarke J P B et al. Continuous descent approach: Design and flight test for Louisville International Airport. *Journal of Aircraft*, Vol. 41, No. 5, pp 1054-1066, 2004

[5] Koenig R and Huemer R G. Noise Saving Potential of Future Approach and Departure Procedures. *Proc. 24th Congr. Int. Council of the Aeronautical Sciences*, paper no. 047, Yokohama, Japan, 2004

[6] Filippone A. Steep-descent Maneuver of Transport Aircraft. *Journal of Aircraft*, Vol. 44, No. 5, pp 1727-1739, 2007

[7] Koenig R, Macke O, and Kreth S. Design and evaluation of short-term realizable new noise abatement flight procedures. *Proc INTER-NOISE 06*, paper no. 266, Honolulu, Hawai, USA, 2006.

[8] Hendriks A. Navigation Developments in Europe. *Proc. FAA New Technologies Workshop III,* Arlington, Virginia, USA, 2007.

[9] Isermann U. *Berechnung der Fluglärmimmission in der Umgebung von Verkehrsflughäfen mit Hilfe eines Simulationsverfahrens.* Dissertation, Universität Göttingen, Germany, 1988.

[10] N.N. *Aviation Noise Effects.* Federal Aviation Administration, 1985

[11] Wimpress J K and Newberry C F. *The YC-14 STOL Prototype: Its Design, Development, and Flight Test*. 1st edition, AIAA, 1998.

[12] McPherson, R L. YC-14 flight test results. *Aircraft Systems and Technology Meeting*, Seattle, Wash., USA, paper no. AIAA-1977-1259, 1977

[13] Norton, B. *STOL Progenitors: The Technology Path to a Large STOL Aircraft and the C-17A*, AIAA, 2002

[14] Horstmann, K-H. *Ein Mehrfach-Traglinien-Verfahren und seine Verwendung für Entwurf und Nachrechnung nichtplanarer Flügelanordnungen.* DFVLR Forschungsbericht 87-51, Institute of Design Aerodynamics of the DFVLR, Braunschweig, Germany, 1987

[15] McCormick, B W. *Aerodynamics of V/STOL Flight*, Dover Publications, 1999

[16] Keen, E B. *A Conceptual Design Methodology for Predicting the Aerodynamics of Upper Surface Blowing on Airfoils and Wings.* Master's Thesis, Virginia Polytechnic Institute & State University, Blacksburg, USA, 2004

[17] Spence, D A. The Lift-Coefficient of a Thin, Jet-Flapped Wing. *Proc. Royal Aeronautical Society*, Series A, Vol. 238, pp 46-68, 1956

[18] Bräunling W J G. *Flugzeugtriebwerke*. 2nd edition, Springer, 2004

[19] Mattingly J D. *Elements of Gas Turbine Propulsion.* McGraw-Hill, 1996

[20] Washington, H P and Gibbons, J T. *Analytical Study of Takeoff and Landing Performance for a Jet STOL Transport Configuration With Full-Span, Externally Blown, Tripple-Slotted Flaps.* NASA-TN-D-7441, 1973.

[21] Yamato H, Okada N and Bando T. Flight Test of the Japanese USB STOL Experimental Aircraft ASKA. *Proc. 4th AIAA Flight Test Conference*, San Diego, California, USA, p. 435-447, 1988.

[22] Korn B, Kuenz, A. 4D FMS for increasing efficiency of tma operations. *Proc. IEEE/AIAA 25th Digital Avionics Systems Conference,* Portland, Oregon, USA, Vols. 1- 3, pp 196-203, 2006.

[23] Macke O and Koenig R. *Comparison of different aircraft noise analysis methods for noise abatement flight procedures.* Proc INTER-NOISE 07, Istanbul, Turkey, paper no. in07_040, 2007.

Copyright Statement